Magnetic and Transport Properties of Fe_4 Single-Molecule Magnets: A Theoretical Insight

Nuria Gallego-Planas,[‡] Alejandro Martín-Rodríguez,[†] Eliseo Ruiz[†*]

[‡] Ingénierie Moléculaire et Matériaux Organiques, UMR 6501, Boulevard Lavoisier, Université d'Angers, F-49045 Angers, France.

[†] Departament de Química Inorgànica i Orgànica and Institut de Química Teòrica i Computacional, Universitat de Barcelona, Diagonal 645, 08028 Barcelona, Spain.

Abstract

Here, methods of density functional theory (DFT) were employed to study the magnetic and transport properties of a star-shaped single-molecule magnet Fe_4 S=5 complex deposited on a gold surface. The study devoted to the magnetic properties focused on changes in the exchange coupling constants and magnetic anisotropy (zero-field splitting parameters) of the isolated and deposited molecules. Molecule-surface interactions induced significant changes in the antiferromagnetic exchange coupling constants because these depend closely on the geometry of the metal complex. Meanwhile, the magnetic anisotropy remained almost constant. Transport properties were analysed using two different approaches. First, we studied the change in the magnetic anisotropy by reducing and oxidizing the Fe_4 complex as in a Coulomb blockade mechanism. Then we studied the coherent tunnelling using DFT methods combined with Green functions. Spin filter behaviour was found because of the different numbers of alpha and beta electrons, due to the S=5 ground state.

Keywords: Density Functional Calculations, Exchange Interactions, Magnetic Anisotropy, Molecular Spintronics, Transport Properties

Introduction

The field of molecular electronics has been developed with the goal of providing miniaturized electronic devices beyond the limits of silicon technology. It has been suggested that the new technologies "More than Moore" and "beyond CMOS"[1] could achieve this in the future and it is clear that heterogeneous devices could replace some silicon components. The use of molecules in such heterogeneous devices could open up new functionalities, especially if magnetic molecules are employed.[2,3] Initially, the combination of molecules and metal surfaces was considered a drawback because in some cases, such as the functionalized single-molecule magnet (SMM) consisting of a Mn_{12} molecule, deposition on the surface was followed by the loss of SMM behaviour due to electron transfer from the surface.[4,5] SMMs are compounds with a relatively large magnetic anisotropy that allows us to fix the spin direction even in the absence of an external magnetic field.[6,7] Thus, they have been proposed for the storage of information at the molecular level. However, recently, in the field of Molecular Spintronics, a new challenge has arisen: to control the electronic structure of the "spinterface" that can provide the combination of molecule+surface system with unexpected new magnetic properties.[2,8] Among others, it is worth to mentioning the magnetic properties of non-magnetic copper or manganese surfaces covered by fullerene molecules under a threshold magnetic field.[9] Also, noteworthy is the spin polarization of the current when injecting electrons from a gold surface to deposited chiral molecules[10-12] or small magnetic molecules[13] at room temperature in single-molecule devices. If the goal is to make devices using molecules showing magnetic anisotropy into SMMs,[14] one of the logical options is to employ molecules that are robust from a chemical point of view;[15] that is, molecules that are more electrochemically stable than the mixed-valence Mn_{12} systems. The two most commonly employed systems are Fe_4 complexes[15-18] and Tb^{III} phthalocyaninate.[19-22] The use of such molecules is relatively new and most of the experiments have been performed far from room conditions; such as in ultrahigh vacuum and at low temperatures. The use of magnetic molecules opens up the possibility of creating new devices for emerging technologies such as those based on spin-transfer

torque mechanisms,[23,24] where the key property is the exchange interaction between the carriers of a spin-polarized current and the spin of the molecule.

Sessoli and coworkers have performed experiments with Fe_4 complexes grafted onto gold surfaces.[15,16,25-30] The magnetic properties of the Fe_4 complexes can be summarized as an S=5 ground state, due to antiferromagnetic coupling between central and terminal Fe^{III} centres, and also as exhibiting small magnetic anisotropy, due to the isotropic d^5 electron configuration of the Fe^{III} cations.[31] Such deposited molecules behave as SMMs, showing hysteresis loops at low temperatures in X-ray Magnetic Circular Dichroism measurements.[15,16,26] More recently, they studied the influence of scanning tunnelling microscopy electrodes on the exchange interactions and found considerable strengthening when the Fe_4 complex is placed in the two-contact junction.[28] The same type of complexes have been studied by the van der Zant and Cornia groups using junction devices to analyse the influence of the electric field on their magnetic properties[18,32,33] and the role of vibron–electron coupling in their transport properties.[17] The analysis of the anisotropy of a single Fe_4 captured between the electrodes indicated that its transverse anisotropy is larger than the bulk-phase value.[34]

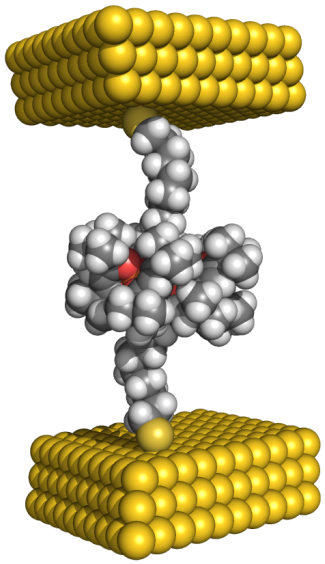

Figure 1. Model structure of the single-molecule Fe_4 device with a sulphur-gold contact to graft the complex to the surface and a long alkyl chain.

Our goal here is to provide a complete theoretical study of the electronic structure, and magnetic and transport properties of SMM Fe_4 complexed on surfaces in order to rationalize our understanding of the properties of single-molecule devices based on such systems (see Fig. 1). The magnitude of the magnetic anisotropy is the key physical parameter for an SMM system, because it determines the height of the spin-flip barrier $D \cdot S^2$, with D being the axial zero-field splitting parameter and S the total spin of the ground state, which depends on polynuclear complexes of the ferromagnetic or antiferromagnetic couplings between the paramagnetic centres. Thus, our study will initially focus on the magnetic properties (exchange interactions and zero-field splitting) of the isolated molecules. The next step will consist of analysis of how such magnetic properties change when the Fe_4 molecules are deposited on gold surfaces. Finally, we will analyse the redox processes involved in a Coulomb blockade regime and their influence on the magnetic anisotropy by considering just the isolated Fe_4 molecule and the transport properties of the coherent tunnelling regime of single-molecule devices with the Fe_4 complexes sandwiched between two gold electrodes (see Fig. 1).

Computational details

Exchange coupling calculations for isolated and deposited Fe_4 complexes were carried out using the SIESTA (Spanish Initiative for Electronic Simulations with Thousands of Atoms) code.[35,36] The code is highly efficient when dealing with systems that contain a large number of atoms and also periodic structures, and therefore for those studied here. The generalized-gradient approximation (GGA) functional expression of Perdew, Burke and Ernzerhof (PBE)[37] was employed and pseudopotentials were generated according to the method suggested by Trouiller and Martins.[38] For the interaction of the Fe_4 molecule with terminal S· radical groups, an S=11 state was considered; due to the long distance between the central Fe_4 and the radical, the ferromagnetic S=11 and

antiferromagnetic S=9 cases are degenerate. For the Fe_4 complex with no ligand functionalization to covalently anchor the gold surface, the DRSLL functional including a dispersion term was employed to optimize the molecule–surface interaction.[39] A triple-ζ numerical basis set with polarization functions for the metal atoms was employed, while a double-ζ basis with polarization functions was used for the other elements. Values of 50 meV for the energy shift and 250 Ry for the mesh cut-off provide a good compromise between accuracy and the computational cost of estimating the exchange coupling constants, according to previous studies[40,41] A detailed description of the procedure used to calculate the exchange coupling constants can be found in previous papers.[42-45] A phenomenological Heisenberg Hamiltonian was used, excluding the terms relating to magnetic anisotropy (*D* and *E* zero-field splitting parameters) to describe the exchange coupling in the polynuclear complex:

$$\hat{H} = -\sum_{a<b} J_{ab} \hat{S}_a \hat{S}_b \qquad (1)$$

where $\hat{S}_a$ and $\hat{S}_b$ are the spin operators of the different paramagnetic centres, and the J_{ab} parameters are the pairwise coupling constants between the paramagnetic centres of the molecule. In general terms, we needed to calculate the energy of n+1 spin distributions for a system with n different exchange coupling constants. In our particular case, only first neighbour exchange interactions of the Fe_4 complexes were considered, thus, depending on the symmetry, there are complexes with from only one to three J values. Thus, for each system, the high spin S=10 spin configuration was calculated and the spin configurations corresponding to the spin-flipping of each terminal Fe^{III} centre directly provided the J value between the terminal and the central Fe^{III} centres. Also, it is worth mentioning that spin-projection approach[42-45] was not included in our calculations. Common exchange-correlations functionals provide good agreement with the experimental data avoiding the double-counting problem of some electronic correlation contribution generated by the

spin-projection method. Due to the large spin of the Fe^{III} centers, the difference in the calculated J value for the inclusion of the spin-projection is only 20%.

The calculation of the zero-field splitting parameters using DFT methods for molecular systems was introduced by Pederson and Khanna.[46] The method introduces the spin–orbit effect through second-order perturbation theory with the following spin-orbit operator:

$$U(r,\mathrm{L},\mathrm{S}) = \frac{1}{2c^2}\mathrm{S}\cdot\mathrm{L}\frac{1}{r}\frac{d\Phi(r)}{dr} \tag{2}$$

where **S** is the spin moment operator, **L** is the angular moment operator, r is the distance and Φ(r) the Coulomb potential operator. V_x matrix elements are then defined as:

$$\left\langle \phi_j \mid V_x \mid \phi_k \right\rangle = \frac{1}{2c^2}\left(\left\langle \frac{d\phi_j}{dz}\middle|\Phi\middle|\frac{d\phi_k}{dy}\right\rangle - \left\langle \frac{d\phi_j}{dy}\middle|\Phi\middle|\frac{d\phi_k}{dz}\right\rangle \right) \tag{3}$$

and second-order perturbative energy can be expressed as:

$$E^{(2)} = \Delta_2 = \sum_{\sigma\sigma'}\sum_{ij} M_{ij}^{\sigma\sigma'} S_i^{\sigma\sigma'} S_j^{\sigma'\sigma} \tag{4}$$

where σ considers all the spins, while i and j correspond to the three spatial directions. The matrix elements are defined as:

$$S_{ij}^{\sigma\sigma'} = \left\langle \chi^{\sigma} \mid S_i \mid \chi^{\sigma'} \right\rangle; \; M_{ij}^{\sigma\sigma'} = -\sum_{kl} \frac{\left\langle \varphi_{l\sigma} \mid V_i \mid \varphi_{k\sigma'} \right\rangle \left\langle \varphi_{k\sigma'} \mid V_j \mid \varphi_{l\sigma} \right\rangle}{\varepsilon_{l\sigma} - \varepsilon_{k\sigma'}} \tag{5}$$

for the full and empty orbitals, respectively, with ε_σ and ε_σ the corresponding energies. Due to the similarity of Eq. 4 with the spin Hamiltonian (Eq. 6), it is possible to compute such a zero-field D value:

$$\hat{H} = \hat{S}\ D\ \hat{S} \tag{6}$$

Thus, for a diagonal form of the tensor, the following expression can be obtained:

$$\sum_{\sigma\sigma'}\sum_{ij} M_{ij}^{\sigma\sigma'} S_i^{\sigma\sigma'} S_j^{\sigma'\sigma} = D_{xx} S_x^2 + D_{yy} S_y^2 + D_{zz} S_z^2 \tag{7}$$

which allows us to obtain each component independently:

$$D_{ii} S_i^2 = \sum_{\sigma\sigma'} M_{ii}^{\sigma\sigma'} S_i^{\sigma\sigma'} S_i^{\sigma'\sigma} \tag{8}$$

Using the most common form of the Hamiltonian:

$$\hat{H} = D\ (\hat{S}_z^2 - \frac{1}{3}\hat{S}^2) + E\ (\hat{S}_x^2 - \hat{S}_y^2) \tag{9}$$

we can obtain the final expression for the D and E zero-field splitting parameters from the diagonal terms of the **D** tensor:

$$D = D_{zz} - \frac{1}{2}(D_{xx} + D_{yy})\ ;\ E = \frac{1}{2}(D_{xx} - D_{yy}) \tag{10}$$

This method was implemented in the NRLMOL code, using the PBE functional and its own basis set. As the calculations are restricted to molecular systems, they were performed on the isolated Fe_4 complexes using the experimental structures.[46-48] For the deposited systems, the molecular structure was taken from the structural optimization with the gold surface, but the zero-field splitting parameters were determined for the molecule alone, without the surface.

Transport calculations were performed using version 3.0 of the SIESTA code[35,36] using the PBE functional[37] with and double-zeta basis set for all the elements, with the exception of gold; for which a single-zeta basis was used combined with a 1-electron pseudopotential.[49] This 1-electron pseudopotential gives incorrect structures if it is employed for geometry optimization but reasonable transport properties in single-point calculations.[50] Transport properties were obtained by post-processing with the Gollum package mapping in a tight-binding Hamiltonian,[51] the DFT Hamiltonian and overlap matrices obtained with SIESTA. The calculations were performed using a GGA+U approach and the PBE functional[37] with a U value of 4.0 eV. The calculations were carried out in a periodic model with the Fe_4 molecule sandwiched between two gold (111) layers.

The most usual approach used to analyse the phase coherent transport in molecular transport junctions is based on the work of Landauer, Imry and Buttiker.[52] The expression for the conductance (G) for a given system with current I and voltage V is:

$$G = \frac{dI}{dV} = 2\frac{e^2}{h}\sum_i T_{ii} \quad (11)$$

where T_{ii}, e and h are the transmission through channel *i*, the electron charge and the Planck's constant, respectively. From a practical point of view, the sum in Eq. 11 is considered in terms of the molecular orbitals of the molecule that can provide an electron pathway channel between the two electrodes. Thus, the analysis of the transmission curves together with the density of states curves allows us to extract the useful information from the molecular orbitals responsible for the electron transport. Qualitatively, such orbitals have to fulfil two requirements: being close in energy to the Fermi level of the electrodes; and the shape of the molecular orbital must be extended through the whole molecule, with strong interactions with the levels of the metal electrodes.[53-55]

DFT calculations using the Gaussian 09 code[56] were performed to analyse the redox processes of the neutral optimized Fe_4 complexes using an all-electron triple-ζ basis set[57] and the B3LYP functional,[58] in order to determine the total spin and the electronic structure of the oxidized and reduced Fe_4 molecules under the Coulomb blockade regime.

Results and Discussion

Exchange interactions in isolated Fe_4 complexes

In order to study the exchange interactions in the family of Fe_4 complexes, we selected six different complexes (see Figure 2)[59-64] and calculated the J values using the PBE functional with the numerical SIESTA code (see Computational details). The calculated J values are in very good agreement with the experimental data (see Table 1), and there is rough correlation between J values and the Fe-O-Fe angles. Similar values were obtained by Lunghi et al.[65] using the hybrid PBE0 functional. The antiferromagnetic nature of the Fe···Fe interactions results in the most stable spin

configuration corresponding to the spin flipping of the central iron atom, with a total S value of 5 matching the experimental data. The J values are too large for us to expect that a structural distortion can reverse the sign of the interaction to ferromagnetic couplings.

Table 1 J values (in cm^{-1}) for the Fe_4 complexes studied, as calculated using DFT and determined experimentally using the geometry of the X-ray diffraction data; and distances in Å and angles in degrees of the parameters relevant for the magnetostructural correlations.

Complex	Fe···Fe	Fe-O-Fe	J_{calc}	J_{exp}
ABOLEI				
J_{12}	3.197	106.0	-20.3	-20.9
J_{13}	3.182	105.5	-18.9	
J_{14}	3.197	106.0	-20.4	
ITAKUJ				
$J_{12} = J_{13} = J_{14}$	3.086	102.9	-21.6	-16.5
MEMKAR				
J_{12}	3.202	106.3	-21.2	-21
J_{13}	3.202	106.2	-16.6	
J_{14}	3.197	106.1	-22.2	
NIPJEC				
J_{12}	3.061	102.2	-18.0	-21
J_{13}	3.092	102.6	-20.5	
J_{14}	3.092	102.6	-20.7	
XUBWIB				
J_{12}	3.066	101.4	-16.4	-15.9
J_{13}	3.068	101.8	-17.7	
J_{14}	3.068	101.8	-17.7	
ICOCIN				
J_{12}	3.078	102.3	-19.3	-15.9
J_{13}	3.073	102.4	-18.3	
J_{14}	3.073	102.4	-18.3	

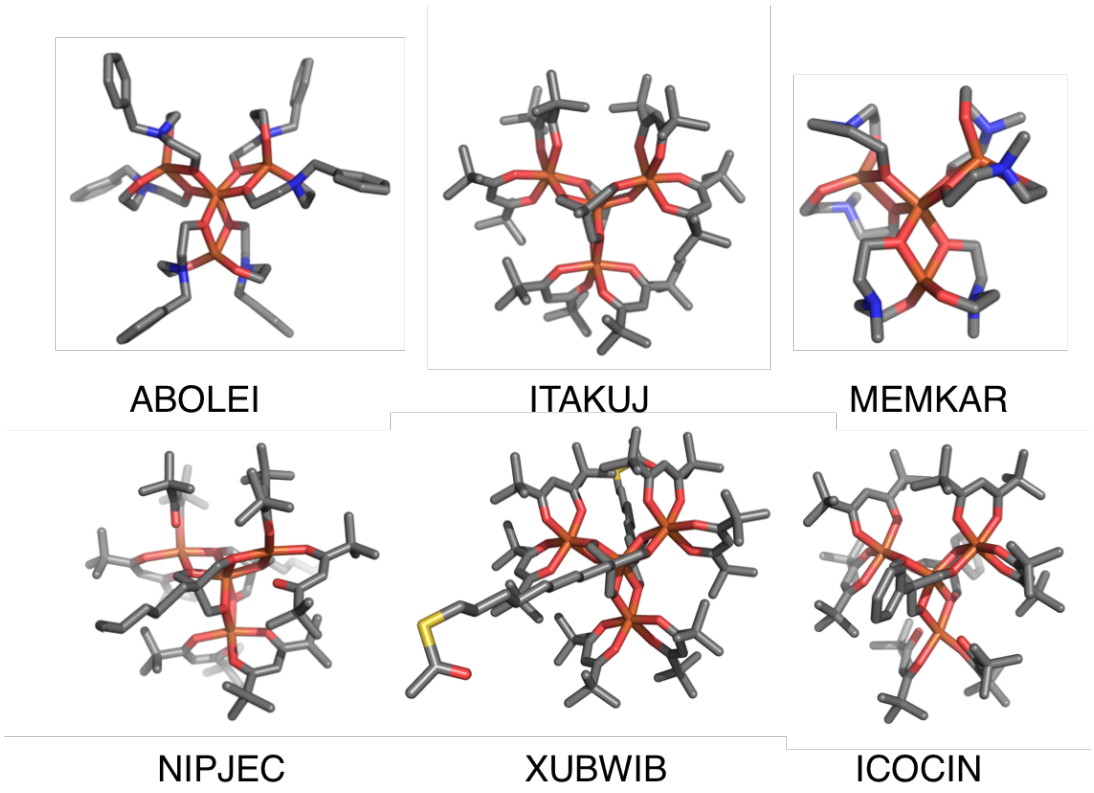

Figure 2. Representation of the six Fe_4 complexes, the label indicates the refcode in the Cambridge Structural Database.[59-64] Orange color corresponds to iron centers while gray, yellow, red and blue are employed for carbon, sulphur, oxygen and nitrogen atoms. ABOLEI: hexakis(μ_2-N-benzyldiethanolamine-N,O,O')-tetra-iron(iii); ITAKUJ: bis(μ_4-1,1,1-tris(oxymethyl)ethane)-hexakis(dipivaloylmethanato)-tetra-iron(iii); MEMKAR: hexakis(μ_2-N,N-bis(2-oxyethyl)methylamido)-tetra-iron(iii); NIPJEC: bis(μ_4-dec-9-ene-1,1,1-trimethanolato-O,O,O',O',O'',O'')-hexakis(1,3-bis(t-butyl)-1,3-propanedionato-O,O')-tetra-iron(iii); XUBWIB: bis(m4-1,1,1-tris(oxymethyl)-10-(acetythio)-n-decane-O,O,O',O',O'',O'')-hexakis(2,2,6,6-tetramethylheptane-3,5-dionato-O,O')-tetra-iron(iii); ICOCIN: bis(μ_4-2-oxymethyl-2-phenyl-1,3-propanediolato)-hexakis(dipivaloylmethanato)-tetra-iron(iii) diethyl ether solvate.

Exchange interactions of Fe_4 complexes deposited on gold surfaces

For the analysis of the variation in the exchange interactions of the Fe_4 complexes with the gold surfaces, two systems were selected: the complexes XUBWIB[60] and ICOCIN[59] (hereafter, Fe_4C9 and Fe_4ph, respectively). There is an important difference between the systems: in Fe_4C9, the ligand functionalization with a thioester group provides efficient anchoring but with a long distance between the central Fe_4 moiety and the surface; while for the Fe4ph system, there are just van der Waals interactions. Due to the long length of the ligands of the Fe_4C9 system, two possible interaction modes with the surface are possible ("standing-up" and "lying-down", see Fig. 3). The

third molecule also employed in the molecular electronics experiments is an equivalent system but with a shorter ligand than Fe_4C9: with only five methylene units (Fe_4C5); thus, only standing-up is possible.[16] For the study of the interaction of the Fe_4C9 complex with the Au(111) surface, we considered two different chemical structures of the anchoring group: (i) the thioester group maintains its structure during the interaction with the surface; and (ii) homolytic cleavage of the S-C bond occurs with the consequent generation of two radicals: Fe4-S· and an acetyl CH_3-C=O. Thus, two free acetyl radicals will form a diacetyl molecule; this is the mechanism that is usually proposed for thiol groups leading to the formation of hydrogen molecules from hydrogen radicals. Optimized DFT structures (see Computational details section) gave an interaction energy of -6.2 and -28.9 kcal/mol for standing-up and lying-down (S-Au bond distances of 2.820 and 2.810 Å with on-top S-Au interaction) respectively, with the interaction keeping the thioester structure; while in the case of the S· radical, there was an enhancement of the interaction strength: -32.1 and -51.4 kcal/mol for the two cases (S-Au bond distances of 2.556 and 2.439 Å with on-top S-Au interaction). Hence, the most stable case corresponds to the lying-down structure (5.7 kcal/mol more stable than standing-up, with radical contacts) and the interaction through the radical groups (87 kcal/mol more stable lying-down with radical contact than with the thioester groups).

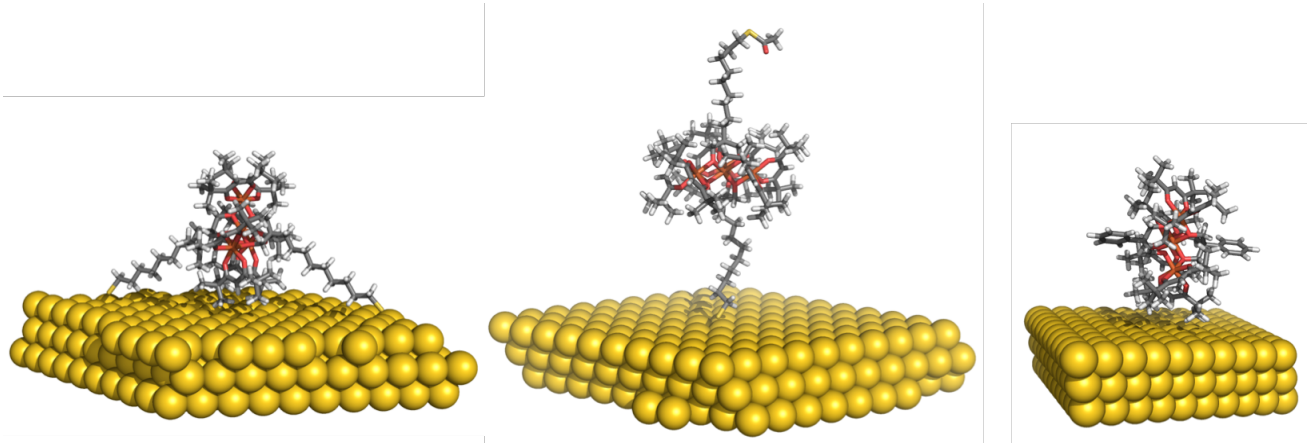

Figure 3. Representation of the Fe_4 complexes deposited on gold surfaces. Two minima were considered for Fe_4C9 (the XUBWIB complex) while the most stable interaction for Fe_4ph (ICOCIN) was with the phenyl ring parallel to the surface, with maximum contact area.

The calculated J values corresponding to the optimized structures of Fe_4C9-Au(111) are reported in Table 2 for the structures with a radical S· anchoring group and the equivalent values for the unchanged thioester ligand. Comparison of the J values with those in Table 1 for the free XUBWIB complex indicate that the interaction with the surface causes a reduction of the antiferromagnetic coupling between the Fe^{III} centres. Despite there being rough correlation between the J values and the Fe-O-Fe angles, the J values obtained for the optimized structures on the surface indicate a general decrease of the Fe-O-Fe angle resulting in a reduction of the strength of the antiferromagnetic Fe···Fe interactions.

Table 2 J values (in cm-1) calculated using DFT and obtained experimentally for the three Fe_4 complexes studied deposited on surfaces (see Fig. 3). In the case of the WUBWIB complex, we considered the formation of a radical in the anchoring thioester group or the original thioester group. For the ICOCIN complex, the values in parenthesis correspond to the optimized isolated molecule. The parameters relevant for the magnetostructural correlations (angles in degrees) are also shown.

Complex	Fe-O-Fe	J_{calc}	Fe-O-Fe	J_{calc}
Fe_4C9 XUBWIB lying-down	radical S·		thioester	
J_{12}	100.3	-10.3	102.1	-7.1
J_{13}	103.0	-16.0	104.7	-13.8
J_{14}	102.8	-15.4	102.0	-14.9
Fe_4C9 XUBWIB standing-up				
J_{12}	101.4	-12.9	99.0	-13.3
J_{13}	103.1	-17.0	102.6	-19.8
J_{14}	102.8	-13.0	103.0	-14.5
Fe_4ph - ICOCIN				
J_{12}	98.0 (100.1)	-3.5 (-10.2)		
J_{13}	97.2 (99.0)	-2.4 (-6.2)		
J_{14}	97.3 (99.0	-3.1 (-6.8)		

In the Fe_4ph (ICOCIN) complex, there are no anchoring groups to attach the molecule to the surface; thus, five different starting orientations were considered in the DFT optimizations and a dispersion term was included in the calculations (see Computational details section) to obtain the structure represented in Figure 3 as the most stable. The phenyl rings are parallel to the gold surface which maximizes the contact between equatorial ligands and the surface, which is 10.1 kcal/mol more stable than the case with one phenyl ring oriented towards the surface. Intermediate tilted orientations of the molecule are much less stable. There is an important change in the structure of the complex due to the interaction with the molecule, but also the optimization of the geometry reduces the bridging angles in comparison with the X-ray data used for the values in Table 1. Such structural modifications are especially important in the case of a considerable decrease in the Fe-O-Fe angle or the antiferromagnetic coupling.

Zero-field splitting parameters of isolated Fe_4 complexes and those deposited on gold surfaces

The magnetic anisotropy of the isolated Fe_4 molecules was studied using DFT methods, including spin–orbit effects (see Table 3). Such an approach usually gives reasonable results for polynuclear complexes with low degeneracy, which allow a realistic description of the ground state with a single Slater determinant.[66] The D value that is often employed to quantify the magnetic anisotropy is correlated with the average of the γ angles between the planes involving the Fe_3 unit (the three external Fe centres) and Fe_2O_2 unit (between the central and the three terminal Fe cations) planes (see Figure 4). This correlation with the γ angle as proposed by Cornia and Sessoli[67,68] is clearly reflected in the D values calculated using DFT. Thus, for the two isolated molecules, the larger angle in NIPJEC is also followed by a slight increase in the D parameter that is in reasonably good agreement with the experimental data in both cases. The E value also increases with the γ angle, but in the optimized DFT structures of the molecule deposited on the gold surface this parameter

becomes larger. This fact should indicate larger tunnelling effects in the spin relaxation for the deposited molecules.

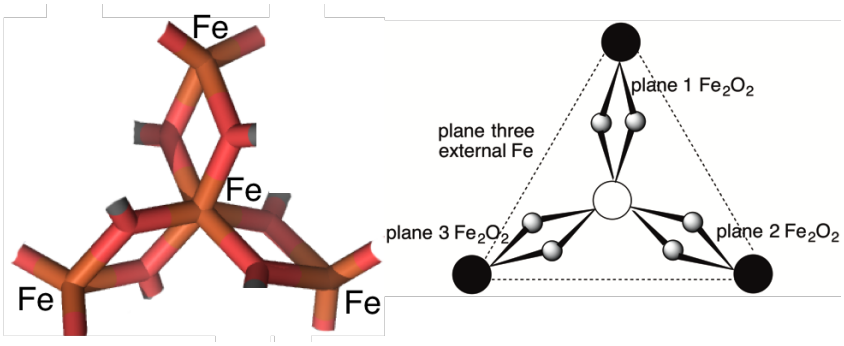

Figure 4. Model structure of a general Fe_4 complex indicating the average γ angle between the planes involving each Fe_3 unit (the three external Fe centres) and the three planes of the Fe_2O_2 units (between the central and the three terminal Fe cations).

Table 3 D(|E|) values (in cm-1) calculated using DFT+SO and experimentally for the isolated Fe_4 complexes with their experimental structures and with the optimized DFT geometrical structure of the molecule deposited on the Au(111) surface indicating the γ angle, which is the key factor in the magnetostructural correlation (angles in degrees). For the deposited molecules, the calculation was performed for the Fe_4 complex alone, but with the optimized DFT structure on the surface (see Computational details section).

Complex	γ	D $(\|E\|)_{calc}$	D $(\|E\|)_{exp}$
Fe_4C9 XUBWIB	67.0	-0.40 (0.005)	-0.412 (0.006)
NIPJEC	69.9	-0.51 (0.01)	-0.434 (0.02)
Fe_4C9 XUBWIB lying-down	65.1	-0.40 (0.035)	
Fe_4C9 XUBWIB standing-up	66.0	-0.42 (0.022)	

Transport properties of single-molecule Fe_4 devices

The transport properties[69,70] of the Fe_4 complexes were studied via two approaches: (i) one assuming a Coulomb blockade mechanism with a molecular redox process associated with the transport that was analysed by comparing DFT results for isolated neutral and charged molecules; and (ii) coherent tunnelling transport was studied using DFT+EGF (see Computational details section) and a model with the Fe_4 complex sandwiched between two periodic gold electrodes.

Magnetic anisotropy controlled the electric field as proposed by Zyazin et al.[18,33,48] is based on the change of the oxidation state of the ICOCIN Fe_4 complex from the S=5 neutral state to a reduced S=11/2 state with a change in the D parameter from -0.06 to -0.09 meV (-0.48 to -0.27 cm^{-1}). We performed DFT calculations using the Gaussian code with the B3LYP functional (see Computational details) to compare the energies of the optimized neutral, reduced and oxidized NIPJEC Fe_4 complex.[62] At first glance, reduction of a Fe_4 complex is expected at the Fe^{III} centres while the S values could be 9/2 or 11/2; while from a chemical point of view, it is expected that the additional electron will cause the reduction of the Fe^{III} cations to give a high-spin S=2 Fe^{II} centre. These predictions were confirmed by the DFT calculations which also showed greater stability of the S=9/2 configuration (around 4843 cm^{-1}) than the S=11/2 case. In the case of the oxidation process, due to the high oxidation state of the Fe^{III} centre, the DFT results indicated that the process occurs on the oxygen atoms of the bridging ligands with a small energy preference for the S=11/2 case (the Fe_4 centres remain unchanged and an additional unpaired alpha electron is delocalized over the ligands). Furthermore, we calculated the D (E) zero-field splitting values for the three cases: the neutral S=5, the reduced S=9/2 and the oxidized S=11/2 NIPJEC Fe4 complex, using the optimized DFT structures; we obtained: -0.40 (0.034), -0.75 (0.007) and +0.47 (0.14) cm^{-1}, respectively. These results clearly corroborate the idea that the electric field can modified the redox state of the Fe_4 complex, as suggested by Zyazin et al.,[18,33] not only by increasing the D value but also the sign of the D value could be changed.

In the second part of this section, the coherent transport properties of the Fe_4 complexes will be analysed with the help of DFT methods. The DFT study was performed using a GGA+U approach using the PBE functional (see Computational details section). The first system that we studied was the Fe_4C9 system with a similar structure to that depicted in Figure 1. However, the capacity of such a system to transport carriers is rather limited due to the long aliphatic chain of the anchoring ligand. For instance, the current calculated for a voltage of 2 V is only 2 pA; thus, we focused on the Fe_4ph system. Hao and coworkers reported a theoretical study of the transport properties using DFT+NEGFT but reducing the length of the Fe_4C9 ligand chain.[71] The transport properties of Fe_4ph system were already studied by adding some thiol groups in the phenyl rings to increase the strength of the molecule–electrode contacts.[72] In our case, we performed the study with the original non-functionalized structure (see Fig. 5) as employed in the experiments.

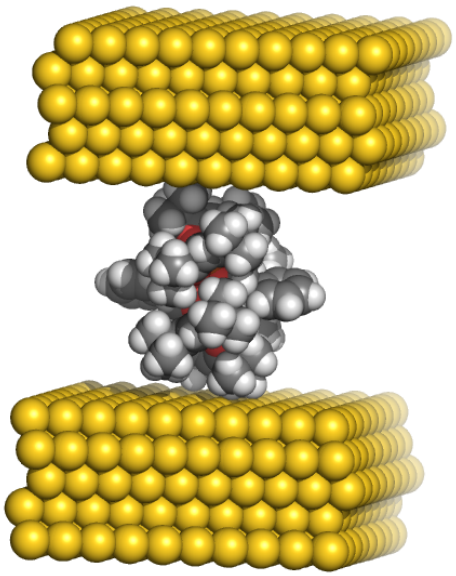

Figure 5. Model structure of the single-molecule Fe_4ph device with the most stable van der Waals interaction between molecule and electrodes determined by DFT calculations in order to maximize the contact area.

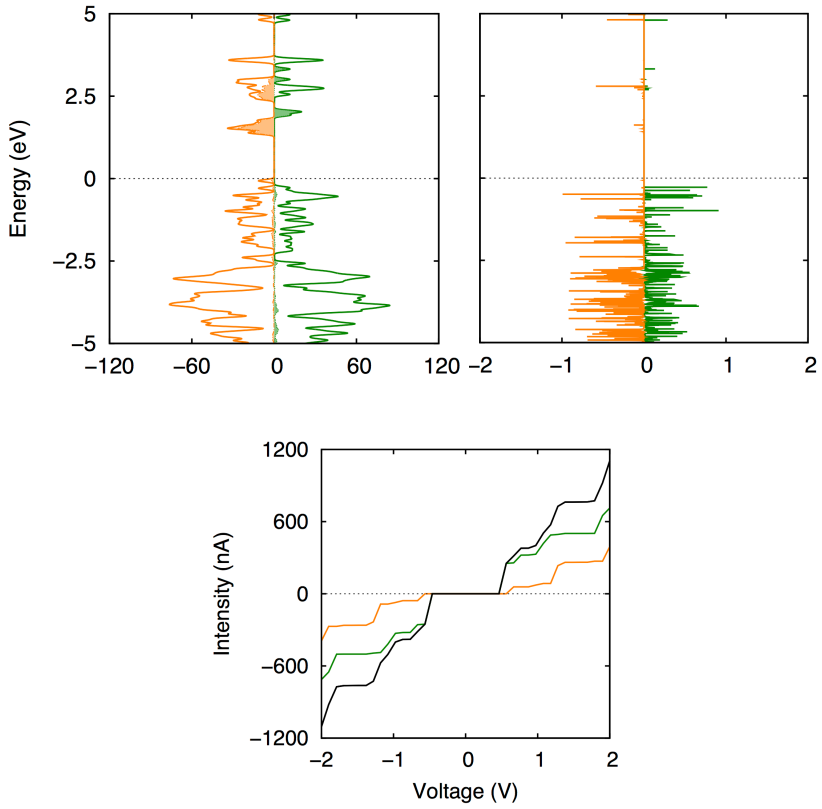

Figure 6. (left) Density of states (DOS) approach. (right) Transmission spectra. (down, middle) I/V characteristics. All calculated with PBE+U (see Computational details). Green and orange colours indicate the alpha and beta contributions. In the DOS representation, filled regions are used to represent the projected Fe contributions; while in the I/V characteristics, the black curve corresponds to the total current.

The results for Fe4ph are shown in Figure 6. The GGA+U provides more accurate results than usual GGA functionals (the geometry was optimised using a functional including dispersion contributions[39]), because it corrects the self-interaction error that causes an underestimation of the energy difference between occupied and empty orbitals. Thus, in Figure 6, the occupied molecular orbitals with a large contribution from the Fe d orbitals are below -5 eV (see DOS) and consequently they are not very important for transport. Empty Fe d orbitals (at +1.5 eV) are closer to the Fermi level but are not relevant for transport, especially at low voltages, when it is mostly

through occupied ligand channels. Thus, we should expect transport mediated mainly by holes and due to the proximity of this level to the Fermi level, relatively low bias will considerably increase the current between the electrodes. The current is slightly spin polarized, with alpha carriers predominant, as can be seen in the transmission spectra where such levels (in green) are closer to the Fermi level than the beta ones. Also, it is worth noting that the current at 2 V is around 1000 nA: several orders of magnitude larger than that found for the Fe_4C9 system; and that despite the almost negligible influence of the Fe d "magnetic" orbitals on the transport properties, a slightly spin-polarized current is obtained due to the influence of such metal orbitals on the ligands.

Concluding Remarks

New spintronic devices based on magnetic molecules face the challenge of the problem of the electronic structure of the spinterface created between the anchored molecule and the surface. In this study, we have analysed changes in the magnetic properties of a family a star Fe_4 complexes showing SMM behaviour when they are deposited on gold surfaces using theoretical methods based on DFT. First, we studied changes in the exchange interactions between the four Fe^{III} cations present in the structures when the molecules were deposited on Au(111) surfaces. These exchange interactions correlated with the Fe-O-Fe bridging angles (larger angles produce stronger antiferromagnetic coupling) and the molecule–surface interaction reduced the bridging angles, resulting in a decrease of the antiferromagnetic couplings.

The second magnetic property that we examined was the magnetic anisotropy by calculating D (and E) zero-field splitting parameters. Magnetic anisotropy is less sensitive to structural changes than exchange coupling constants are, thus, molecule–surface interactions cause only small variations in the calculated D values. The D value correlated, as previously reported, with the average γ angle between the planes involving the Fe_3 unit (the three external Fe centres) and Fe_2O_2 unit (between the central and the three terminal Fe cations) planes. It is worth noting that

despite the small E values calculated, as this magnitude is related to the strength of the spin relaxation tunnelling effects, these should be more important when the molecule is deposited on the surface. This result is in agreement with the common experimentally observed tendency of SMMs to reduce their blocking temperature (or lose the hysteresis loop) when deposited. Furthermore, some spin–phonon relaxation due to the vibrations of the surface will also decrease SMM behaviour.

The transport properties of the Fe_4 complexes were also analysed: firstly, by considering a Coulomb blockade regime where the charge carriers are "captured" by the molecule for a long time period that will imply a change in the oxidation state of the molecule and geometrical rearrangement. The reduction and oxidation processes of one S=5 Fe_4 complex were also studied using DFT methods and showed that in the reduction process, the extra electron is placed at the iron centres (reducing their oxidation state) and as the alpha Fe^{III} d orbitals are completely filled, the electron must be in a beta orbital, resulting in a most stable S=9/2 state. In the oxidation process, as the Fe^{III} centres are already in a high oxidation state, the bridging oxygen atoms lose one electron and for such a case, the S=11/2 state is the most stable. The magnetic anisotropy (D zero-field splitting) was calculated for the neutral, oxidized and reduced complexes showing an important variation of the D values not only in magnitude but even in the sign (changing from easy-axis to easy-plane for the oxidized structure). This result is quite important because it confirms that an electric field employed to reduce or oxidize the molecule can control the magnetic anisotropy of the system.

Finally, the coherent transport properties for the Fe_4ph complex between gold electrodes were analysed in detail using periodic DFT methods combined with Green functions. The results indicated a very low participation of the transport channels involving a large contribution of the Fe^{III} d orbitals, which are not close to the Fermi level. Despite such small contributions of the

"magnetic orbitals" of the molecule, the transport (I/V characteristics) showed a spin polarization due to the influence of these orbitals on those of the ligands. The occupied alpha orbitals of the ligands are mostly responsible for the current; thus, positive carriers should be expected and they could be experimentally corroborated by measuring the thermoelectric effect.

Acknowledgements

The research reported here was supported by the Spanish *Ministerio de Economía y Competitividad* (grant CTQ2015-64579-C3-1-P, MINECO/FEDER, UE). E.R. thanks Generalitat de Catalunya for an ICREA Academia award. A. M.-R. acknowledges the University of Barcelona for a collaboration grant. We. thankfully acknowledge the computer resources in the Barcelona Supercomputer Center, technical expertise and assistance provided by the Red Española de Supercomputación.

References

1. A. Chen, J. Hutchby, V. Zhirnov and G. Bourianoff, eds., *Emerging Nanoelectronic Devices*, WIley, Chichester, 2015.
2. S. Sanvito, *Nat Phys*, 2010, **6**, 562.
3. S. Sanvito, *Chem. Soc. Rev.*, 2011, **40**, 3336.
4. A. Cornia, A. C. Fabretti, M. Pacchioni, L. Zobbi, D. Bonacchi, A. Caneschi, D. Gatteschi, R. Biagi, U. Del Pennino, V. De Renzi, L. Gurevich and H. S. J. Van der Zant, *Angew. Chem. Int. Ed.*, 2003, **42**, 1645.
5. A. Naitabdi, J. P. Bucher, P. Gerbier, P. Rabu and M. Drillon, *Adv. Mater.*, 2005, **17**, 1612.
6. D. Gatteschi and R. Sessoli, *Angew. Chem. Int. Ed.*, 2003, **42**, 268.
7. D. Gatteschi, R. Sessoli and J. Villain, *Molecular Nanomagnets*, Oxford University Press, Oxford, 2006.
8. M. Galbiati, S. Tatay, C. Barraud, A. V. Dediu, F. Petroff, R. Mattana and P. Seneor, *MRS Bull.*, 2014, **39**, 602.
9. F. A. Ma/'Mari, T. Moorsom, G. Teobaldi, W. Deacon, T. Prokscha, H. Luetkens, S. Lee, G. E. Sterbinsky, D. A. Arena, D. A. MacLaren, M. Flokstra, M. Ali, M. C. Wheeler, G. Burnell, B. J. Hickey and O. Cespedes, *Nature*, 2015, **524**, 69.
10. B. Göhler, V. Hamelbeck, T. Z. Markus, M. Kettner, G. F. Hanne, Z. Vager, R. Naaman and H. Zacharias, *Science*, 2011, **331**, 894.
11. R. Naaman and Z. Vager, *Phys. Chem. Chem. Phys.*, 2006, **8**, 2217.
12. R. Naaman and D. H. Waldeck, in *Annual Review of Physical Chemistry, Vol 66*, eds. M. A. Johnson and T. J. Martinez, 2015, vol. 66, pp. 263.
13. A. C. Aragonès, D. Aravena, J. I. Cerdá, Z. Acís-Castillo, H. Li, J. A. Real, F. Sanz, J. Hihath, E. Ruiz and I. Díez-Pérez, *Nano Lett.*, 2015.

14. A. Canneschi, D. Gatteschi, F. Totti, *Coord. Chem. Rev.*, 2015, **289-290**, 357.
15. M. Mannini, F. Pineider, P. Sainctavit, C. Danieli, E. Otero, C. Sciancalepore, A. M. Talarico, M.-A. Arrio, A. Cornia, D. Gatteschi and R. Sessoli, *Nat. Mat.*, 2009, **8**, 194.
16. M. Mannini, F. Pineider, C. Danieli, F. Totti, L. Sorace, P. Sainctavit, M. A. Arrio, E. Otero, L. Joly, J. C. Cezar, A. Cornia and R. Sessoli, *Nature*, 2010, **468**, 417.
17. E. Burzuri, Y. Yamamoto, M. Warnock, X. Zhong, K. Park, A. Cornia and H. S. J. van der Zant, *Nano Lett.*, 2014, **14**, 3191.
18. A. S. Zyazin, J. W. G. van den Berg, E. A. Osorio, H. S. J. van der Zant, N. P. Konstantinidis, M. Leijnse, M. R. Wegewijs, F. May, W. Hofstetter, C. Danieli and A. Cornia, *Nano Lett.*, 2010, **10**, 3307.
19. R. Vincent, S. Klyatskaya, M. Ruben, W. Wernsdorfer and F. Balestro, *Nature*, 2012, **488**, 357.
20. J. Schwobel, Y. S. Fu, J. Brede, A. Dilullo, G. Hoffmann, S. Klyatskaya, M. Ruben and R. Wiesendanger, *Nat. Commun.*, 2012, **3**.
21. M. Urdampilleta, S. Klyatskaya, J. P. Cleuziou, M. Ruben and W. Wernsdorfer, *Nat. Mat.*, 2011, **10**, 502.
22. S. Wagner, F. Kisslinger, S. Ballmann, F. Schramm, R. Chandrasekar, T. Bodenstein, O. Fuhr, D. Secker, K. Fink, M. Ruben and H. B. Weber, *Nat. Nanotech.*, 2013, **8**, 575.
23. S. H. Kang, *JOM*, 2008, **60**, 28.
24. L. Jiang, X. Liu, Z. Zhang and R. Wang, *Phys. Lett. A*, 2014, **378**, 426.
25. F. Pineider, M. Mannini, C. Danieli, L. Armelao, F. M. Piras, A. Magnani, A. Cornia and R. Sessoli, *J. Mater. Chem.*, 2010, **20**, 187.
26. M. Mannini, E. Tancini, L. Sorace, P. Sainctavit, M.-A. Arrio, Y. Qian, E. Otero, D. Chiappe, L. Margheriti, J. C. Cezar, R. Sessoli and A. Cornia, *Inorg. Chem.*, 2011, **50**, 2911.
27. M. Perfetti, F. Pineider, L. Poggini, E. Otero, M. Mannini, L. Sorace, C. Sangregorio, A. Cornia and R. Sessoli, *Small*, 2014, **10**, 323.
28. J. A. J. Burgess, L. Malavolti, V. Lanzilotto, M. Mannini, S. Yan, S. Ninova, F. Totti, S. Rolf-Pissarczyk, A. Cornia, R. Sessoli and S. Loth, *Nat. Commun.*, 2015, **6**.
29. A. Lunghi, M. Iannuzzi, R. Sessoli and F. Totti, *J. Mate. Chem. C*, 2015, **3**, 7294.
30. L. Malavolti, V. Lanzilotto, S. Ninova, L. Poggini, I. Cimatti, B. Cortigiani, L. Margheriti, D. Chiappe, E. Otero, P. Sainctavit, F. Totti, A. Cornia, M. Mannini and R. Sessoli, *Nano Lett.*, 2015, **15**, 535.
31. A. L. Barra, A. Caneschi, A. Cornia, F. F. de Biani, D. Gatteschi, C. Sangregorio, R. Sessoli and L. Sorace, *J. Am. Chem. Soc.*, 1999, **121**, 5302.
32. E. Burzuri, A. S. Zyazin, A. Cornia and H. S. J. van der Zant, *Phys. Rev. Lett.*, 2012, **109**, 147203.
33. A. S. Zyazin, H. S. J. van der Zant, M. R. Wegewijs and A. Cornia, *Synth. Met.*, 2011, **161**, 591.
34. M. Misiorny, E. Burzuri, R. Gaudenzi, K. Park, M. Leijnse, M. R. Wegewijs, J. Paaske, A. Cornia and H. S. J. van der Zant, *Phys. Rev. B*, 2015, **91**, 035442.
35. J. M. Soler, E. Artacho, J. D. Gale, A. Garcia, J. Junquera, P. Ordejon and D. Sanchez-Portal, *J. Phys-Cond. Matter*, 2002, **14**, 2745.
36. D. Sánchez-Portal, P. Ordejón and E. Canadell, in *Principles and Applications of Density Functional Theory in Inorganic Chemistry II*, Springer Berlin Heidelberg, Berlin, Heidelberg, 2004, pp. 103.
37. J. P. Perdew, K. Burke and M. Ernzerhof, *Phys. Rev. Lett.*, 1996, **77**, 3865.
38. N. Trouiller and J. L. Martins, *Phys. Rev. B*, 1991, **43**, 1993.
39. M. Dion, H. Rydberg, E. Schroder, D. C. Langreth and B. I. Lundqvist, *Phys. Rev. Lett.*, 2004, **92**, 246401.

40. E. Ruiz, A. Rodríguez-Fortea, J. Tercero, T. Cauchy and C. Massobrio, *J. Chem. Phys.*, 2005, **123**, 074102.
41. E. Ruiz, T. Cauchy, J. Cano, R. Costa, J. Tercero and S. Alvarez, *J. Am. Chem. Soc.*, 2008, **130**, 7420.
42. E. Ruiz, A. Rodríguez-Fortea, J. Cano, S. Alvarez and P. Alemany, *J. Comput. Chem.*, 2003, **24**, 982.
43. E. Ruiz, J. Cano, S. Alvarez and P. Alemany, *J. Comput. Chem.*, 1999, **20**, 1391.
44. E. Ruiz, P. Alemany, S. Alvarez and J. Cano, *J. Am. Chem. Soc.*, 1997, **119**, 1297.
45. E. Ruiz, *J. Comput. Chem.*, 2011, **32**, 1998.
46. M. R. Pederson and S. N. Khanna, *Phys. Rev. B*, 1999, **60**, 9566.
47. J. Ribas-Arino, T. Baruah and M. R. Pederson, *J. Chem. Phys.*, 2005, **123**, 044303.
48. A. McCaskey, Y. Yamamoto, M. Warnock, E. Burzurí, H. S. J. van der Zant and K. Park, *Phys. Rev. B*, 2015, **91**, 125419.
49. M. Brandbyge, J. L. Mozos, P. Ordejon, J. Taylor and K. Stokbro, *Phys. Rev. B*, 2002, **65**, 165401.
50. C. Toher and S. Sanvito, *Phys. Rev. B*, 2008, **77**, 155402.
51. J. Ferrer, C. J. Lambert, V. M. Garcia-Suarez, D. Z. Manrique, D. Visontai, L. Oroszlany, R. Rodriguez-Ferradas, I. Grace, S. W. D. Bailey, K. Gillemot, H. Sadeghi and L. A. Algharagholy, *New. J. Phys.*, 2014, **16**, 093029.
52. M. Buttiker, Y. Imry, R. Landauer and S. Pinhas, *Phys. Rev. B*, 1985, **31**, 6207.
53. D. Aravena and E. Ruiz, *J. Am. Chem. Soc.*, 2011, **134**, 777.
54. E. Ruiz, *Phys. Chem. Chem. Phys.*, 2014, **16**, 14.
55. E. Cremades, C. D. Pemmaraju, S. Sanvito and E. Ruiz, *Nanoscale*, 2013, **5**, 4751.
56. Gaussion 09 (release D.01) M. J. Frisch, G. W. Trucks, H. B. Schlegel, G. E. Scuseria, M. A. Robb, J. R. Cheeseman, G. Scalmani, V. Barone, B. Mennucci, G. A. Petersson, H. Nakatsuji, M. Caricato, X. Li, H. P. Hratchian, A. F. Izmaylov, J. Bloino, G. Zheng, J. L. Sonnenberg, M. Hada, M. Ehara, K. Toyota, R. Fukuda, J. Hasegawa, M. Ishida, T. Nakajima, Y. Honda, O. Kitao, H. Nakai, T. Vreven, J. Montgomery, J. A., J. E. Peralta, F. Ogliaro, M. Bearpark, J. J. Heyd, E. Brothers, K. N. Kudin, V. N. Staroverov, R. Kobayashi, J. Normand, K. Raghavachari, A. Rendell, J. C. Burant, S. S. Iyengar, J. Tomasi, M. Cossi, N. Rega, N. J. Millam, M. Klene, J. E. Knox, J. B. Cross, V. Bakken, C. Adamo, J. Jaramillo, R. Gomperts, R. E. Stratmann, O. Yazyev, A. J. Austin, R. Cammi, C. Pomelli, J. W. Ochterski, R. L. Martin, K. Morokuma, V. G. Zakrzewski, G. A. Voth, P. Salvador, J. J. Dannenberg, S. Dapprich, A. D. Daniels, Ö. Farkas, J. B. Foresman, J. V. Ortiz, J. Cioslowski and D. J. Fox, Wallingford, CT, 2009.
57. A. Schafer, C. Huber and R. Ahlrichs, *J. Chem. Phys.*, 1994, **100**, 5829.
58. A. D. Becke, *J. Chem. Phys.*, 1993, **98**, 5648.
59. S. Accorsi, A.-L. Barra, A. Caneschi, G. Chastanet, A. Cornia, A. C. Fabretti, D. Gatteschi, C. Mortalo, E. Olivieri, F. Parenti, P. Rosa, R. Sessoli, L. Sorace, W. Wernsdorfer and L. Zobbi, *J. Am. Chem. Soc.*, 2006, **128**, 4742.
60. L. Gregoli, C. Danieli, A.-L. Barra, P. Neugebauer, G. Pellegrino, G. Poneti, R. Sessoli and A. Cornia, *Chem.-Eur.J.*, 2009, **15**, 6456.
61. A. Cornia, A. C. Fabretti, P. Garrisi, C. Mortalo, D. Bonacchi, D. Gatteschi, R. Sessoli, L. Sorace, W.Wernsdorfer and A.-L. Barra, *Angew. Chem.,Int. Ed.*, 2004, **43**, 1136.
62. A.-L. Barra, F. Bianchi, A. Caneschi, A. Cornia, D. Gatteschi, L. Gorini, L.Gregoli, M. Maffini, F. Parenti, R. Sessoli, L. Sorace and A. M. Talarico, *Eur. J. Inorg.Chem.*, 2007, 4145.
63. R. W. Saalfrank, I. Bernt, M. M. Chowdhry, F. Hampel and G. B. M.Vaughan, *Chem.-Eur.J.*, 2001, **7**, 2765.

64. R. W. Saalfrank, A. Scheurer, I. Bernt, F. W. Heinemann, A. V. Postnikov, V. Schunemann, A. X. Trautwein, M. S. Alam, H. Rupp and P. Muller, *Dalton Trans.*, 2006, 2865.
65. A. Lunghi and F. Totti, *J. Mater. Chem. C*, 2014, **2**, 8333.
66. M. Atanasov, D. Aravena, E. Suturina, E. Bill, D. Maganas and F. Neese, *Coord. Chem. Rev.*, 2015, **289**, 177.
67. S. Accorsi, A. L. Barra, A. Caneschi, G. Chastanet, A. Cornia, A. C. Fabretti, D. Gatteschi, C. Mortalo, E. Olivieri, F. Parenti, P. Rosa, R. Sessoli, L. Sorace, W. Wernsdorfer and L. Zobbi, *J. Am. Chem. Soc.*, 2006, **128**, 4742.
68. L. Gregoli, C. Danieli, A.-L. Barra, P. Neugebauer, G. Pellegrino, G. Poneti, R. Sessoli and A. Cornia, *Chem. Eur. J.*, 2009, **15**, 6456.
69. M. Di Ventra and Moscato Book Fund, *Electrical transport in nanoscale systems*, Cambridge University Press, Cambridge, UK ; New York, 2008.
70. K. Hirose and N. Kobayashi, *Quantum Transport Calculations for Nanosystems*, Pan Stanford Publishing, Singapore, 2014.
71. H. Hao, X. Zheng, T. Jia and Z. Zeng, *RSC Adv.*, 2015, **5**, 54667.
72. F. Zu, Z. Liu, K. Yao, G. Gao, H. Fu, S. Zhu, Y. Ni and L. Peng, *Sci. Rep.*, 2014, **4**, 4838.